

AD-A157 435

THE USE OF WALL-COATED CELLS IN ATOMIC FREQUENCY
STANDARDS(U) AEROSPACE CORP EL SEGUNDO CA CHEMISTRY AND
PHYSICS LAB R P FRUEHOLZ ET AL. 24 JUN 85
TR-0084A(5945-05)-5 SD-TR-85-18

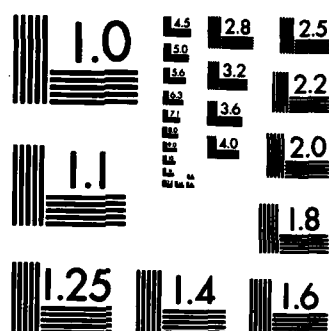
1/1

UNCLASSIFIED

F/G 14/2

NL





MICROCOPY RESOLUTION TEST CHART
NATIONAL BUREAU OF STANDARDS-1963-A

2

AD-A157 435

The Use of Wall-Coated Cells in Atomic Frequency Standards

R. P. FRUEHOLZ, C. H. VOLK, and J. C. CAMPARO
✓Chemistry and Physics Laboratory
Laboratory Operations
The Aerospace Corporation
El Segundo, CA 90245

24 June 1985

APPROVED FOR PUBLIC RELEASE;
DISTRIBUTION UNLIMITED

DTIC FILE COPY

Prepared for
SPACE DIVISION
AIR FORCE SYSTEMS COMMAND
Los Angeles Air Force Station
P.O. Box 92960, Worldway Postal Center
Los Angeles, CA 90009-2960

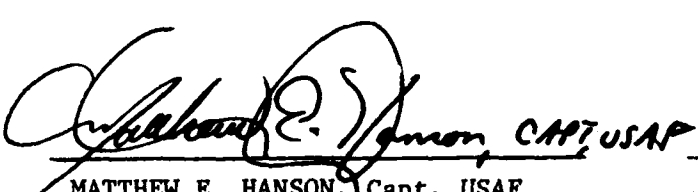
DTIC
ELECTE
AUG 2 1985

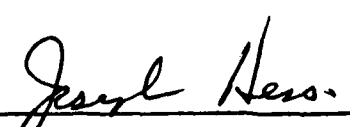
85 7 23 042

This report was submitted by The Aerospace Corporation, El Segundo, CA 90245, under Contract No. F04701-83-C-0084 with the Space Division, P.O. Box 92960, Worldway Postal Center, Los Angeles, CA 90009. It was reviewed and approved or The Aerospace Corporation by S. Feuerstein, Director, Chemistry and Physics Laboratory. Capt Matthew E. Hanson, SD/YEZ, was the project officer for the Mission-Oriented Investigation and Experimentation (MOIE) Program.

This report has been reviewed by the Public Affairs Office (PAS) and is releasable to the National Technical Information Service (NTIS). At NTIS, it will be available to the general public, including foreign nationals.

This technical report has been reviewed and is approved for publication. Publication of this report does not constitute Air Force approval of the report's findings or conclusions. It is published only for the exchange and stimulation of ideas.


MATTHEW E. HANSON, Capt, USAF
Ch, Satellite Development Branch
SD/YEZ


JOSEPH HESS, GM-15
Director, AFSTC West Coast Office
AFSTC/WCO OL-AB

UNCLASSIFIED

SECURITY CLASSIFICATION OF THIS PAGE (When Data Entered)

REPORT DOCUMENTATION PAGE		READ INSTRUCTIONS BEFORE COMPLETING FORM
1. REPORT NUMBER SD-TR-85-18	2. GOVT ACCESSION NO. AD-A157435	3. REPORT'S CATALOG NUMBER
4. TITLE (and Subtitle) THE USE OF WALL-COATED CELLS IN ATOMIC FREQUENCY STANDARDS		5. TYPE OF REPORT & PERIOD COVERED
7. AUTHOR(s) Robert P. Frueholz, Charles H. Volk, and James C. Camparo		6. PERFORMING ORG. REPORT NUMBER TR-0084A(5945-05)-5
9. PERFORMING ORGANIZATION NAME AND ADDRESS The Aerospace Corporation El Segundo, Calif. 90245		8. CONTRACT OR GRANT NUMBER(s) F04701-83-C-0084
11. CONTROLLING OFFICE NAME AND ADDRESS Space Division Los Angeles Air Force Station Los Angeles, Calif. 90009-2960		10. PROGRAM ELEMENT, PROJECT, TASK AREA & WORK UNIT NUMBERS
14. MONITORING AGENCY NAME & ADDRESS (if different from Controlling Office)		12. REPORT DATE 24 June 1985
		13. NUMBER OF PAGES 21
		15. SECURITY CLASS. (of this report) Unclassified
		15a. DECLASSIFICATION/DOWNGRADING SCHEDULE
16. DISTRIBUTION STATEMENT (of this Report) Approved for public release; distribution unlimited.		
17. DISTRIBUTION STATEMENT (of the abstract entered in Block 20, if different from Report)		
18. SUPPLEMENTARY NOTES		
19. KEY WORDS (Continue on reverse side if necessary and identify by block number) Atomic clocks; Atomic line shapes; Motional narrowing. <i>← eval</i>		
20. ABSTRACT (Continue on reverse side if necessary and identify by block number) An analysis of the effect of the microwave field distribution on the application of a wall-coated, bufferless absorption cell in an atomic frequency standard has been performed. While certain advantages of using such a cell in an atomic frequency standard employing a TE ₀₁₁ microwave cavity have been previously demonstrated, we show that a simple incorporation of this type of cell in a frequency standard using a TE ₀₁₁ microwave cavity would not be advantageous. The role of the microwave field distribution, <i>sub 111</i> <i>sub 211</i>		

DD FORM 1473
(FACSIMILE)

UNCLASSIFIED

SECURITY CLASSIFICATION OF THIS PAGE (When Data Entered)

19. KEY WORDS (Continued)

20. ABSTRACT (Continued)

particularly its phase variation within the cavity, is analyzed, and suggestions concerning the use of a wall-coated cell in a TE₁₁₁ microwave cavity as applied to an atomic frequency standard are made.

sub 11'

Keywords
↓
shielding

Discussion For

THIS CASE



THIS CASE



Advanced



Classification

A-1



CONTENTS

I.	INTRODUCTION.....	3
II.	DISCUSSION.....	5
	A. Dicke Narrowing in a TE_{111} Microwave Cavity.....	5
	B. Dicke Narrowing in the TE_{011} Cavity.....	14
III.	CONCLUSIONS.....	19
	REFERENCES	21

FIGURES

Fig. 1.	Phase of the z Component of the Magnetic Field in a Right Cylindrical Cavity, TE_{111} Mode.....	8
Fig. 2.	$\cos(\eta)$ Value as a Function of Time for an Atom Moving Freely in the Microwave Cavity.....	11
Fig. 3.	Phase of the z Component of the Magnetic Field in a Right Cylindrical Cavity, TE_{011} Mode.....	15
Fig. 4.	Normalized Hyperfine Lineshapes for Wall-Coated Cells in Cavities Operating in TE_{011} and TE_{111} Modes.....	17

I. INTRODUCTION

It has been known for some time that there are particular advantages to using hydrocarbon coatings on the absorption cell walls for the optical pumping of alkali vapors.¹ Recent work has been directed toward applying such a wall-coated cell in a rubidium gas cell atomic clock.^{2,3} An advantage of the wall-coated cell in the atomic clock is that this type of cell does not require a buffer gas, because wall collisions in the coated cell have only a weak effect on the alkali spin.¹ One of the unfortunate consequences of using a buffer gas in the conventional clock cell is that the atoms cannot average the various local gradients such as those due to magnetic field, the pumping light, etc., which then results in an asymmetric microwave absorption line. Because of the inhomogeneous nature of the microwave absorption line, the clock is sensitive to microwave power fluctuations, and this leads to potential instabilities in the clock's performance. Published results² have shown that with the elimination of the buffer gas and the use of a wall-coated cell in a TE_{011} microwave cavity, a rubidium clock can be made greatly insensitive to microwave power fluctuations.

In an attempt to make the rubidium clock more compact and thus easier to incorporate into various practical applications, many manufacturers have started using the TE_{111} microwave cavity, because it is small compared to the TE_{011} cavity.⁴ In this report we consider the incorporation of a wall-coated, bufferless absorption cell in a TE_{111} cavity for use in a frequency standard. We show that simple replacement of the presently used buffered cell with a bufferless, wall-coated cell is not sufficient for high-performance clock operation. The resonance signal from such a cell in a TE_{111} cavity will have a broad linewidth compared to the typical Dicke-narrowed resonance, and this will result in a frequency standard with a degraded Q. However, if such a cell is used in a TE_{011} cavity, the Q is not degraded, and all the advantages of a wall-coated cell may be realized. Although these facts have been experimentally known to investigators familiar with the operation of the

hydrogen maser, previous analyses of this phenomenon are found to be incomplete. These analyses took advantage of various physical design features of the maser. The analysis presented here relaxes these constraints to give a more complete description of the line-broadening phenomenon in the TE_{111} cavity.

II. DISCUSSION

The fundamental operation of a passive, gas-cell atomic frequency standard involves the detection of an atomic microwave transition, which is then used as a reference to stabilize the frequency of a quartz crystal oscillator. Typically an alkali vapor, e.g. rubidium, is used, and a population imbalance between the ground-state hyperfine energy levels is created by optically pumping the gas sample. Detection of the microwave transition is accomplished by monitoring the light intensity transmitted through an absorption cell within a microwave cavity. The frequency stability that can be achieved by locking a crystal oscillator to an atomic transition depends on the Q of the atomic transition⁵ and thus on the atomic linewidth. Contributions to the linewidth include the pumping radiation; collisions with other atoms in the alkali ensemble, with foreign gas atoms, and with the cell walls; the microwave field; magnetic inhomogeneities; and Doppler broadening.

It was Dicke⁶ who first pointed out that Doppler broadening could be made negligibly small if a radiating atom's mean free path is small compared to the emitted photon's wavelength. In the gas-cell clock, reduction of the Doppler contribution results in a linewidth of approximately 500 Hz, compared to a normal Doppler width of about 10 kHz. To limit the atom's mean free path, a nonmagnetic buffer gas is typically used in the absorption cell.⁷ It is important that a nonmagnetic (inert) buffer is used, since collisions between the alkali atoms and these inert buffer atoms will cause relatively little change in the internal state of the alkali atoms; i.e., phase changes associated with these collisions can be neglected. To analyze the effect of using a wall-coated, bufferless absorption cell in an atomic clock, we derive the Dicke line shape for the case in which the atoms experience an effective phase shift as a result of their motion relative to the microwave field distribution.

A. DICKE NARROWING IN A TE_{111} MICROWAVE CAVITY

Dicke narrowing has been studied in detail by several authors.^{8,9} A convenient approach is to consider the radiating atomic system, in our case

the rubidium ensemble, as a collection of classical oscillators. The displacement for any oscillator can be written as

$$x(\tau) = A \cos\left[\int_0^{\tau} \omega'(t) dt\right] \quad (1)$$

A is taken to be proportional to the value of the component of the electromagnetic field, which induces the oscillation, averaged over the spatial region to which the oscillator is confined. Assuming that phase changes induced by collisions are negligible, the oscillator's instantaneous frequency, $\omega'(t)$, can be written as

$$\omega'(t) = \omega_0 + \beta(t) \omega_0 \quad (2)$$

where β is the ratio of the z component of the velocity to the speed of light. The autocorrelation function of the displacement is written as

$$F(\tau) = \langle x(\tau) \cdot x(0) \rangle \quad (3)$$

where the brackets in Eq. (3) represent an averaging over collision times and postcollision velocities. The Fourier transform of the autocorrelation function yields the oscillator's spectral density, which classically is equivalent to the atomic line shape. $F(\tau)$ can be written in the form

$$F(\tau) = \frac{A^2}{2} \operatorname{Re}\left[e^{i\omega_0\tau} f(\tau)\right] \quad (4)$$

where Re indicates that the real part of the function is to be taken, and $f(\tau)$ is termed the reduced autocorrelation function, given by

$$f(\tau) = \langle \exp[i\omega_0 \int_0^{\tau} \beta(t) dt] \rangle \quad (5)$$

Gersten and Foley⁸ have shown that in the limit the mean free path, $\bar{\ell}$, is much less than the wavelength of the emitted photon, λ_0 . The Fourier transform of Eq. (4) results in a spectral density function, $G(\omega)$, with the typical Dicke-narrowed Lorentzian dependence:

$$G(\omega) \propto \frac{\Gamma}{\Gamma^2 + (\omega - \omega_0)^2} \quad (6)$$

where the half width, Γ , is approximately one percent of the Doppler half width.⁶

One of the assumptions implicit in this analysis has been that the atomic oscillators are always in phase with any interrogating microwave field. This assumption is satisfied for atoms in a buffered cell because they are collisionally confined to regions of nearly constant phase. A similar situation exists in certain hydrogen masers in which the atoms are confined by the walls of the resonance cell to a region of constant phase. For the hydrogen maser, an approximate line shape analysis under the restrictive assumption of constant phase was performed by Kleppner et al.¹⁰ However, in the wall-coated, bufferless cells of interest for use in rubidium frequency standards, the atoms move about the entire cavity volume. Consequently, they can experience effective phase shifts associated with their motion relative to the microwave field. This more general line shape problem, including the effects of motionally induced phase changes, is treated in this report.

The component of oscillating field that stimulates the rubidium 0-0 hyperfine transition is H_z , where z is taken along the quantization axis (which in the usual situation corresponds to the cylindrical axis of the cell). The phase of H_z in a cylindrical TE_{111} cavity is shown in Fig. 1. As can be seen, there is a phase change of π radians dividing the cylindrical volume in half. From the atom's point of view, as it moves across this boundary it goes from a condition of being in phase with the microwave field to a condition of being out of phase with the microwave field. This is not to be taken as an instantaneous loss of phase coherence, because the oscillator ensemble will maintain this coherence over a time T_2 . However, there is an

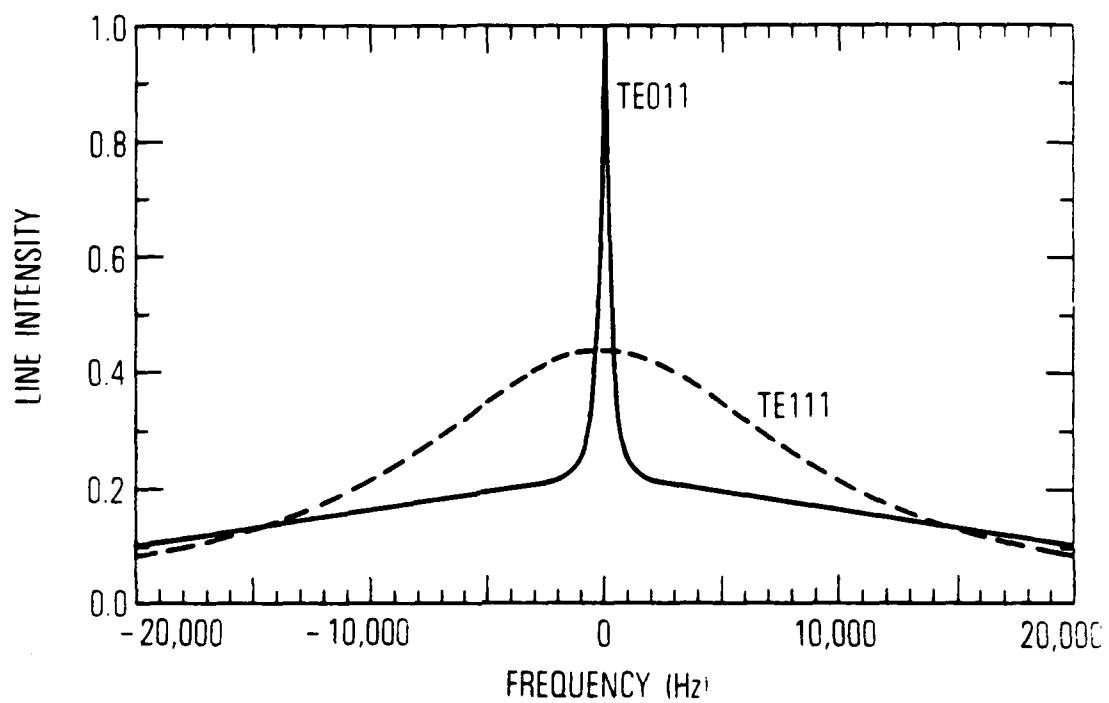


Fig. 1. Phase of the z Component of the Magnetic Field in a Right Cylindrical Cavity, TE₁₁₁ Mode.

instantaneous phase change with respect to the driving field as the atom crosses a nodal surface of the field.

To incorporate a phase shift of this type, we follow the lead of Gersten and Foley, adding an additional phase-shift variable, $\eta(\tau)$, to the displacement term:

$$x(\tau) = A \cos\left[\int_0^\tau \omega'(t) dt + \eta(\tau)\right] \quad (7)$$

In our analysis $\eta(\tau)$ then represents the difference in phase between the atom and the field. As the atom moves from a region of one phase to another, $\eta(\tau)$ instantaneously changes by π , and the oscillator's displacement with respect to the field changes sign. The exact form of the temporal behavior of $\eta(\tau)$ after this instantaneous change will be discussed subsequently. The reduced autocorrelation function now takes the form

$$f(\tau) = \langle \exp[i\omega_0 \int_0^\tau \beta(t) dt + \eta(\tau) + \eta(0)] \rangle \quad (8)$$

with an additional average over $\eta(\tau)$ implied. Since $\eta(\tau)$ is independent of $\beta(t)$, which is assumed to randomize after each collision, averages over η and β may be performed independently. We thus have

$$f(\tau) = \{ \langle \exp[i\omega_0 \int_0^\tau \beta(t) dt] \rangle \} \langle \cos[\eta(\tau)] \cos[\eta(0)] \rangle \quad (9)$$

where η is constrained to take on the values of 0 and π only. Through Eq. (9) the effects of motionally induced phase changes have been separated from the standard Dicke-narrowed line shape. This allows close inspection of the phase-change effects. In the subsequent analysis the Dicke-narrowed line shape is assumed to be a pure Lorentzian. A more complicated line shape, including a small residual Doppler component, could easily be treated.

In evaluating $\langle \cos[\eta(\tau)] \rangle$ we define two regimes of microwave power. First, the case of high microwave power: as the atom moves from a region of + to - phase, η changes from 0 to π . Subsequently, in this intense field the atomic oscillator will rapidly rephase with the field, resulting in η going to

zero. Then, as the atom moves back from a - region to a + region, η will again jump from 0 to π and then rephase rapidly to zero before the atom has a chance to leave that region of phase. The second situation is what we term low microwave power, in which the atomic oscillator's phase is negligibly affected by the cavity phase change. As the atom moves from a region of + to - phase, η again jumps from 0 to π . However, because the microwave field is weak, there is no significant rephasing of the atom with respect to the microwave field, and thus η remains π until the atom returns to a + cavity phase region. Because the atom is now in phase with the field, η returns to zero.

Atomic gas-cell clocks typically operate in the low microwave power regime, as defined above. In this power regime, $\cos[\eta(\tau)]$ takes on the values ± 1 . The changes from one value to the other are essentially random as a result of the velocity distribution and random-walk trajectory that the atom follows. We estimate the average number of sign flips of the cosine function per unit time, $1/t_r$, as the average velocity of the atoms in the cell, \bar{v} , divided by the cell radius, R_c :

$$1/t_r = \frac{\bar{v}}{R_c} \quad (10)$$

For the commonly used cell size in a TE_{111} cavity this works out to be about $3 \times 10^4 \text{ sec}^{-1}$. The probability of $\cos[\eta(\tau)]$ having either value, ± 1 , is just given by the ratio of the cell volume with the phase yielding the particular value of $\cos[\eta(\tau)]$ to the total cell volume. For the TE_{111} cavity, which has equal regions of + and - phase, the probabilities are both equal to $\frac{1}{2}$.

The values of $\cos[\eta(\tau)]$ as a function of time can be pictured in Fig. 2. Since the length of time the function takes on one value or the other is controlled by the random walk of the atom, we can take the probability that k phase changes occur in a time interval T as given by the Poisson distribution

$$P(k, T) = \frac{(a T)^k}{k!} \exp(-aT) \quad (11)$$

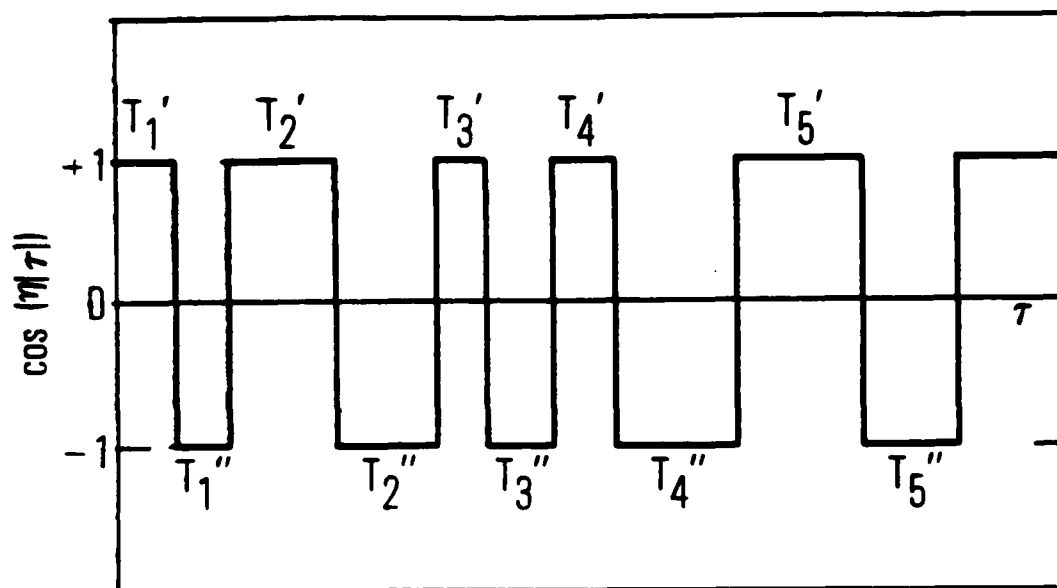


Fig. 2. $\cos(\eta)$ Value as a Function of Time for an Atom Moving Freely in the Microwave Cavity. For the TE_{111} mode the single- and double-primed times are distributed according to a single Poisson distribution. For the TE_{011} mode, the single- and double-primed times are distributed according to different Poisson distributions.

where a is the average number of traversals per unit time. Within this approximation we may apply the analysis presented by Davenport and Root¹¹ to calculate the autocorrelation function, $R(\tau)$, of $\cos[n(\tau)]$. $R(\tau)$ is defined to be

$$R(\tau) = \langle \cos[n(\tau)] \cdot \cos[n(0)] \rangle \quad (12)$$

$\cos[n(\tau)]$ and $\cos[n(0)]$ are each discrete random variables that we designate as x_1 and x_2 , respectively. From Ref. (11) we can write

$$\begin{aligned} R(\tau) = & (-1 \cdot -1)P(x_1 = -1, x_2 = -1) + (-1 \cdot 1)P(x_1 = -1, x_2 = 1) \\ & + (1 \cdot -1)P(x_1 = 1, x_2 = -1) + (1 \cdot 1)P(x_1 = 1, x_2 = 1) \end{aligned} \quad (13)$$

where $P(x_1 = a, x_2 = b)$ is the probability that x_1 has the value a and x_2 has the value b . The probability that x_1 and x_2 have the same value is just the probability that x_1 has a particular value and that the atom has undergone an even number of traversals in a time τ .

Similarly, the probability that x_1 and x_2 have different values is the probability that x_1 has a particular value and that the atom has undergone an odd number of traversals in time. Thus

$$\begin{aligned} P(x_1 = 1, x_2 = 1) &= P(x_1 = -1, x_2 = -1) = P(x_1 = 1, k \text{ even}) \\ &= P(x_1 = 1) \cdot P(k \text{ even}) \end{aligned} \quad (14a)$$

and

$$\begin{aligned} P(x_1 = 1, x_2 = -1) &= P(x_1 = -1, x_2 = 1) = P(x_1 = 1, k \text{ odd}) \\ &= P(x_1 = 1) \cdot P(k \text{ odd}) \end{aligned} \quad (14b)$$

Using the Poisson distribution and after some straightforward calculations, the autocorrelation function is found to be

$$R(\tau) = \exp(-2a |\tau|) \quad (15)$$

To obtain the spectral density, we take the Fourier transform of Eq. (4), with $f(\tau)$ now given by Eq. (9). Equation (9) is the product of Gersten and Foley's result and the autocorrelation function given in Eq. (15). Applying the Fourier transform convolution theorem, we need to compute the Fourier transforms of both autocorrelation functions and convolve the result to obtain the total spectral density. The spectral density of the autocorrelation function given in Eq. (15), $S(\omega)$, is found to be

$$S(\omega) \propto \frac{a}{4a^2 + (\omega - \omega_0)^2} \quad (16)$$

Equation (16) is seen to be in the form of a Lorentzian function, as was the case with $G(\omega)$. The convolution of two Lorentzian functions results in a Lorentzian function. The spectral density $I(\omega)$ is found by convolving $G(\omega)$ and $S(\omega)$ so that

$$I(\omega) = \int_{-\infty}^{\infty} G(\omega - \phi) S(\phi) d\phi \quad (17)$$

Performing the convolution we find

$$I(\omega) \propto \frac{1}{\frac{(\Gamma_{\text{Dicke}} + \Gamma_{\text{phase}})^2}{4} + (\omega - \omega_0)^2} \quad (18)$$

where $\Gamma_{\text{Dicke}} = 2\Gamma$ and $\Gamma_{\text{phase}} = 4a$. We define the Dicke-narrowed linewidth to be the full linewidth in the presence of Dicke narrowing, not simply the "residual" Dicke linewidth; i.e., this linewidth has contributions from effects such as collisional broadening, light broadening, and the like.

The resulting Lorentzian has a linewidth of $\Gamma_{\text{Dicke}} + \Gamma_{\text{phase}}$. A typical Dicke-narrowed linewidth is about 500 Hz. Using parameters for commonly used clock cells, we estimate $\Gamma_{\text{phase}} = 19$ kHz. The effect of the reversal of the cavity phase in the TE_{111} cavity is to increase the linewidth from about 500 Hz to nearly 20 kHz. This linewidth would result in clock performance seriously degraded from that presently obtained with buffered cells in a TE_{111} cavity.

B. DICKE NARROWING IN THE TE_{011} CAVITY

Although a similar reversal in phase of the cavity field exists in the TE_{011} cavity, narrow linewidths have been obtained by using wall-coated, bufferless absorption cells.² To analyze this situation we consider the phase distribution in the TE_{011} cavity, shown in Fig. 3. The reversal in phase in this cavity is in the radial direction, and the phase-change surface does not divide the cell into equal volumes. The region of + phase occupies about 39% of the volume, while the region of - phase is about 61% of the total cell volume. We will demonstrate that it is the nonequal phase volumes that allow the Dicke-narrowed linewidth to be obtained.

To analyze the nonequal-volume phase regions, several approximations must be made. Since the probability of being in either phase region, P_+ or P_- , is directly proportional to that region's fraction of the total cavity volume, we then assume that the average time in a phase region, t_i , can be taken to be

$$t_i = \frac{V_i}{V_t} \cdot t_r \quad i = +, - \quad (19)$$

where V_i is the volume corresponding to a particular phase region, and V_t is the total volume of the cavity. The reciprocal of t_i , denoted as ρ_i , can be considered as the average rate of transition from phase region i to the other phase region. We can treat the effective atomic phase fluctuations in this type of cavity as an "alternating Poisson process."¹² The probabilities of leaving each phase region are taken to be independent Poisson distributions.

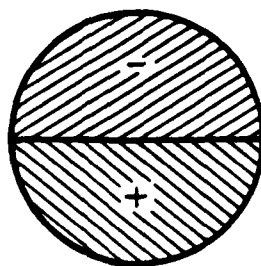


Fig. 3. Phase of the z Component of the Magnetic Field in a Right Cylindrical Cavity, TE_{011} Mode.

Using the analysis in Ref. (12), the autocorrelation function indicated in Eq. (12) may be calculated for the TE_{011} cavity, so that

$$R(\tau) = (P_+ - P_-) \times \frac{(\rho_- - \rho_+)}{(\rho_- + \rho_+)} - 2 \frac{[P_+\rho_- + P_-\rho_+]}{\rho_+ + \rho_-} e^{-(\rho_+ + \rho_-)\tau} \quad (20)$$

This autocorrelation function, shown explicitly in Eq. (20), must again be multiplied by the result of Gersten and Foley, as in Eq. (9).

The total autocorrelation function for the TE_{011} cavity differs from that for the TE_{111} cavity in that it is composed of two terms, an exponential term similar to that found for the TE_{111} cavity and, additionally, a constant term. The resulting line shape is then composed of two parts: first, a broadly smeared Lorentzian, as was found in the TE_{111} case; secondly, a Dicke-narrowed peak, which is what is normally observed in buffered cells. The Dicke narrowed peak would be the predominant feature, since the broadened line would have its intensity spread over a large frequency range. For the typical situation, the Dicke-narrowed peak for the wall-coated bufferless cell in the TE_{011} cavity would have a narrower line shape than that for a buffered cell, because atoms in the former cell would be able to motionally narrow effects caused by inhomogeneous broadening. Figure 4 shows the calculated line shapes for both the TE_{111} and TE_{011} cavity modes.

Finally, we can consider the case in which the microwave power is increased in the TE_{111} cavity so that atoms crossing the phase boundary are immediately rephased with respect to the field. This would imply that the atoms would spend more time in phase than out, and thus a Dicke-narrowed line shape should be produced. In this case, however, microwave power broadening would be significant and would have to be taken into consideration. If the rephasing time were equal to the atomic transit time, the uncertainty principle would predict a linewidth given by

$$\Delta\nu \approx \frac{1}{2\pi t_r} = 9 \text{ kHz}$$

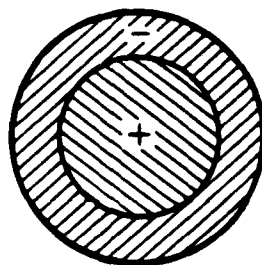


Fig. 4. Normalized Hyperfine Line Shapes for Wall-Coated Cells in Cavities Operating in TE_{011} and TE_{111} Modes.

This linewidth is seen to be much larger than typical linewidths in rubidium clocks, which would imply that a clock operated in this manner would have a degraded performance compared to a clock operated normally.

IV. CONCLUSIONS

In wall-coated cells, just as in buffer-gas-filled cells, the collisional constraints required for Dicke narrowing can be met. However, in the former the free movement of atoms throughout the entire microwave cavity introduces additional complications to line-shape analysis. The preceding investigation determined the effects of this free atomic motion on the rubidium's hyperfine line shape. It was concluded that when treating the atom as a classical oscillator, one must consider the atom's phase with respect to the phase of the cavity fields.

In general, cavities in which the average occupation times of each phase region are the same will yield line shapes significantly broader than the Dicke limit. Conversely, cavities in which the mean occupation times of the phase volumes are not equal will display line shapes composed of two components, a broadened Lorentzian and a superimposed Dicke-narrowed Lorentzian. Specifically, in a TE_{111} cavity direct insertion of a wall-coated cell without buffer gas will result in a broadened hyperfine line shape and degraded frequency-standard performance. However, a similar insertion of a wall-coated cell into a TE_{011} cavity, with its unequal phase regions, would not only yield a Dicke-narrowed line but also reduce effects of inhomogeneous broadening through motional averaging.

In light of the TE_{011} results, the use of a wall-coated cell in the TE_{111} cavity need not be precluded entirely. Phase changing caused by atomic motion could be eliminated by separating the two regions with some partition.¹³ Alternatively, an asymmetric cell would yield nonequal phase-region occupancy times, also resulting in a Dicke-narrowed line.

REFERENCES

1. M. A. Bouchiat and J. Brossel, Phys. Rev. 147, 41 (1966).
2. A. Risley, S. Jarvis, and J. Vanier, J. Appl. Phys. 51, 4571 (1980).
3. H. G. Robinson and C. E. Johnson, Appl. Phys. Lett. 40, 771 (1982).
4. E. Jechart, Proceedings of the 2nd Annual Frequency Control Symposium, U.S. Army Electronics Command, Fort Monmouth, N.J. (1973), pp. 387-389.
5. J. Vanier, R. Kunski, A. Brisson, and P. Paulin, J. de Physique 12, C8-139 (1981).
6. R. H. Dicke, Phys. Rev. 89, 472 (1953); R. H. Romer and R. H. Dicke, Phys. Rev. 99, 532 (1955).
7. J. M. Andres, D. J. Farmer, and G. T. Inouye, IRE Trans. Mil. Elec. MIL-3, 178 (1959); M. Arditi and T. R. Carver, Phys. Rev. 124, 800 (1961); M. Arditi and T. R. Carver, Phys. Rev. 126, A643 (1964); C. W. Beer and R. A. Bernheim, Phys. Rev. A13, 1052 (1974); G. Missout and J. Vanier, IEEE Trans. Instru. and Meas. 24, 180 (1975); J. Vanier, D. H. Nguyen, G. Busca, and M. Tetu, Can. J. of Phys. 57, 1380 (1979); J. Vanier, R. Kunski, N. Cyr, J. Y. Savard, and M. Tetu, J. Appl. Phys. 53, 5387 (1982).
8. J. I. Gersten and H. M. Foley, J. Opt. Soc. Am. 58, 933 (1968).
9. L. Galatry, Phys. Rev. 122, 1218 (1961).
10. D. Kleppner, H. M. Goldenberg, and N. F. Ramsey, Phys. Rev. 126, 603 (1962).
11. W. B. Davenport and W. L. Root, An Introduction to the Theory of Random Signals, (McGraw Hill Book Co., Inc., New York, N.Y., 1958), p. 61.
12. D. R. Cox and H. D. Miller, The Theory of Stochastic Processes, (John Wiley and Sons, Inc., New York, N.Y., 1965), p. 350.
13. E. M. Mattison, M. W. Levine, and R. F. C. Vessot, Proceedings of the 8th Precise Time and Time-Interval Applications and Planning Meeting, Washington, D.C., (1976) p. 355.

LABORATORY OPERATIONS

The Laboratory Operations of The Aerospace Corporation is conducting experimental and theoretical investigations necessary for the evaluation and application of scientific advances to new military space systems. Versatility and flexibility have been developed to a high degree by the laboratory personnel in dealing with the many problems encountered in the nation's rapidly developing space systems. Expertise in the latest scientific developments is vital to the accomplishment of tasks related to these problems. The laboratories that contribute to this research are:

Aerophysics Laboratory: Launch vehicle and reentry fluid mechanics, heat transfer and flight dynamics; chemical and electric propulsion, propellant chemistry, environmental hazards, trace detection; spacecraft structural mechanics, contamination, thermal and structural control; high temperature thermomechanics, gas kinetics and radiation; cw and pulsed laser development including chemical kinetics, spectroscopy, optical resonators, beam control, atmospheric propagation, laser effects and countermeasures.

Chemistry and Physics Laboratory: Atmospheric chemical reactions, atmospheric optics, light scattering, state-specific chemical reactions and radiation transport in rocket plumes, applied laser spectroscopy, laser chemistry, laser optoelectronics, solar cell physics, battery electrochemistry, space vacuum and radiation effects on materials, lubrication and surface phenomena, thermionic emission, photosensitive materials and detectors, atomic frequency standards, and environmental chemistry.

Computer Science Laboratory: Program verification, program translation, performance-sensitive system design, distributed architectures for spaceborne computers, fault-tolerant computer systems, artificial intelligence and microelectronics applications.

Electronics Research Laboratory: Microelectronics, GaAs low noise and power devices, semiconductor lasers, electromagnetic and optical propagation phenomena, quantum electronics, laser communications, lidar, and electro-optics; communication sciences, applied electronics, semiconductor crystal and device physics, radiometric imaging; millimeter wave, microwave technology, and RF systems research.

Materials Sciences Laboratory: Development of new materials: metal matrix composites, polymers, and new forms of carbon; nondestructive evaluation, component failure analysis and reliability; fracture mechanics and stress corrosion; analysis and evaluation of materials at cryogenic and elevated temperatures as well as in space and enemy-induced environments.

Space Sciences Laboratory: Magnetospheric, auroral and cosmic ray physics, wave-particle interactions, magnetospheric plasma waves; atmospheric and ionospheric physics, density and composition of the upper atmosphere, remote sensing using atmospheric radiation; solar physics, infrared astronomy, infrared signature analysis; effects of solar activity, magnetic storms and nuclear explosions on the earth's atmosphere, ionosphere and magnetosphere; effects of electromagnetic and particulate radiations on space systems; space instrumentation.

END

FILMED

9-85

DTIC